

# A Federated Learning-Friendly Approach for Parameter-Efficient Fine-Tuning of SAM in 3D Segmentation

Mothilal Asokan , Joseph Geo Benjamin  , Mohammad Yaqub , and Karthik Nandakumar 

Mohamed bin Zayed University of Artificial Intelligence (MBZUAI),  
Abu Dhabi, United Arab Emirates  
{mothilal.asokan, joseph.benjamin, mohammad.yaqub,  
karthik.nandakumar}@mbzuai.ac.ae

**Abstract.** Adapting foundation models for medical image analysis requires finetuning them on a considerable amount of data because of extreme distribution shifts between natural (source) data used for pretraining and medical (target) data. However, collecting task-specific medical data for such finetuning at a central location raises many privacy concerns. Although Federated learning (FL) provides an effective means for training on private decentralized data, communication costs in federating large foundation models can quickly become a significant bottleneck, impacting the solution’s scalability. In this work, we address this problem of ‘efficient communication while ensuring effective learning in FL’ by combining the strengths of Parameter-Efficient Fine-tuning (PEFT) with FL. Specifically, we study plug-and-play Low-Rank Adapters (LoRA) in a federated manner to adapt the Segment Anything Model (SAM) for 3D medical image segmentation. Unlike prior works that utilize LoRA and finetune the entire decoder, we critically analyze the contribution of each granular component of SAM on finetuning performance. Thus, we identify specific layers to be federated that are very efficient in terms of communication cost while producing on-par accuracy. Our experiments show that retaining the parameters of the SAM model (including most of the decoder) in their original state during adaptation is beneficial because fine-tuning on small datasets tends to distort the inherent capabilities of the underlying foundation model. On Fed-KiTS, our approach decreases communication cost ( $\sim 48\times$   $\downarrow$ ) compared to full fine-tuning while increasing performance ( $\sim 6\%$   $\uparrow$  Dice score) in 3D segmentation tasks. Our approach performs similar to SAMed while achieving  $\sim 2.8\times$  reduction in communication and parameters to be finetuned. We further validate our approach with experiments on Fed-IXI and Prostate MRI datasets. Our code is available at <https://github.com/BioMedIA-MBZUAI/FLAP-SAM>.

**Keywords:** Federated Learning · Foundation Model · 3D Medical Image Segmentation · Parameter-Efficient Fine-Tuning

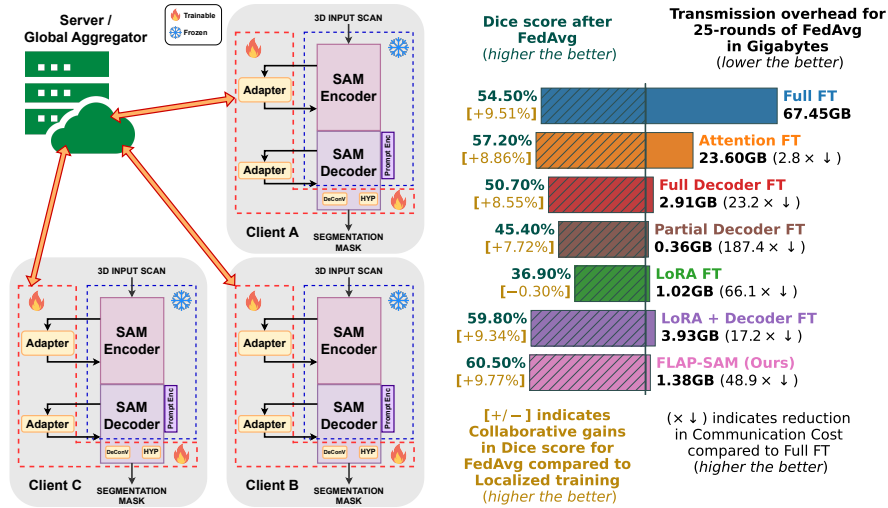


**Fig. 1.** (Left) The proposed FLAP-SAM framework and (Right). The comparison (in terms of Dice score(%), Collaborative gains(%) and Communication Cost( $\times \downarrow$ )) of our method against other fine-tuning methods on Fed-KITS2019[26].

## 1 Introduction

Segmentation is one of the cornerstone tasks in modern medical image analysis for automated diagnosis and disease monitoring. While the advent of foundational models has pushed the boundaries of the state-of-the-art in many computer vision applications, such benefits are yet to transfer fully to the medical imaging domain [33]. For example, the Segment Anything Model (SAM) [14] has an excellent zero-shot generalization to new distributions and tasks involving natural images. However, the SAM model fails to generalize well across diverse medical imaging modalities due to the insurmountable distribution shifts [11]. Works like [6,10] highlight a substantial performance gap between the zero-shot inference and training on domain-specific medical images despite using various prompts in SAM. MSA [29] and SAM-Med2D [4] improve SAM by using tailored prompting techniques in 2D medical images. However, creating such prompts for each 2D slice of 3D data is labor-intensive.

The usual approach has been fine-tuning SAM for the target application using large task-specific datasets e.g., MedSAM[20]. For tasks with significant distribution shifts with limited data, the decoder block of SAM is fine-tuned while leaving the encoder untouched. In contrast to fine-tuning all parameters, parameter-efficient fine-tuning (PEFT) methods fine-tune only a minimal number of parameters using representative data such as prompt tuning [12] and low-rank adapters (LoRA) [9]. Several works [22,28,32] have employed LoRA for fine-tuning, resulting in superior performance in various 2D segmentation tasks. For 3d segmentation, [2] uses factor tuning (FacT) adapters [13] for training.

However, accessing diverse medical data for such finetuning is not always feasible because relevant datasets specific to a medical task may not be available with any single entity. It is often spread across multiple institutions and cannot be shared due to privacy and confidentiality constraints [26]. While the data decentralization issue can be handled effectively with federated learning (FL) [21,16], the ginormous parameter size of SAM ( $\sim 100\text{M}-700\text{M}$ ) makes it impractical for FL as it imposes a substantial communication cost.

In this work, we uncover the importance of fine-tuning various components of SAM when adapted for 3D medical segmentation and propose **FLAP-SAM**, a *PEFT approach involving LoRA that is amenable to FL* (see Fig 1). Moreover, high parameter efficiency reduces communication costs in FL and prevents overfitting in data-limited scenarios. With methods like MA-SAM[2], which uses FacT adapters for 3D segmentation, it is challenging to federate because of the tensor decomposition involved. Hence, we employ LoRA, which is FL-friendly, to customize SAM for 3D medical image segmentation. SAMed[32] uses a similar approach where LoRA and the entire SAM decoder are fine-tuned for 2D segmentation. Our approach selectively finetunes certain decoder parts, reducing parameters and communication costs.

## 2 Preliminaries

**Overview of SAM:** The architecture of SAM[14] can be decoupled into three major components: the *Image Encoder* (IE) to compute image embeddings, the *Prompt Encoder* (PE) to generate prompt embeddings, and the *Mask Decoder* (MD) that combines the image and prompt embeddings to generate segmentation masks as shown in Fig 2. Utilizing ViT [5] as the backbone, IE extracts image features through a sequence of  $L$  transformer blocks. Meanwhile, PE takes various input prompts in the form of points, boxes, or masks and encodes them into prompt embeddings to aid in segmentation tasks. We operate SAM in the *fully automatic* mode, in which a regular grid of foreground points is presented as input prompts to the PE, thus eliminating the dependence on user-defined prompts. MD performs cross-attention between the image and prompt embeddings, employing transposed convolutional layers for up-scaling back to image dimension (UP) and a hyper multi-layer perceptron (HYP) to produce segmentation masks. Following [2], we use a slightly modified SAM mask decoder that has two additional transposed convolutional layers, which up-sample the feature maps by  $16\times$  to match the resolution of the input while ensuring improved discrimination of small anatomical structures or lesions in medical images [24].

For simplicity, let  $\theta_{\text{IE}}$ ,  $\theta_{\text{PE}}$ , and  $\theta_{\text{MD}}$  denote the parameters of IE, PE, and MD, respectively. Also,  $\theta_{\text{IE}}$  can be further partitioned as  $\theta_{\text{IE-AT}}$  and  $\theta_{\text{IE-NA}}$ , where  $\theta_{\text{IE-AT}}$  denotes the parameters of all the attention layers within IE and  $\theta_{\text{IE-NA}}$  represents all the other parameters in IE not related to the attention layers. On the other hand,  $\theta_{\text{MD}}$  can be partitioned as  $\theta_{\text{MD-TR}}$ ,  $\theta_{\text{MD-UP}}$ , and  $\theta_{\text{MD-HYP}}$ , where  $\theta_{\text{MD-TR}}$  denotes the parameters of all the transformer blocks within MD (such as self-attention, cross-attention from tokens to image embeddings (t2i), and cross-

attention from image embeddings to tokens (i2t)),  $\theta_{\text{MD-UP}}$  denotes the parameters of the transposed convolutional layers used for upscaling, and  $\theta_{\text{MD-HYP}}$  represents the parameters of HYP.

**PEFT Formulation:** The most straightforward approach to adapt a SAM model for a downstream task is to fine-tune all its parameters, including  $\theta_{\text{IE}}$ ,  $\theta_{\text{PE}}$ , and  $\theta_{\text{MD}}$ . This full fine-tuning (FullFT) strategy requires more memory footprint to store a copy of all the updated parameters and often leads to overfitting when the data is severely limited. Recent works have shown that fine-tuning only the attention layers of a transformer encoder is sufficient for good adaptation [27]. This approach is called attention fine-tuning (AttnFT), where only  $\theta_{\text{IE-AT}}$  and  $\theta_{\text{MD}}$  are updated. Typically, the attention-related parameters of a transformer encoder constitute one-third of its overall parameters. Thus, AttnFT leads to some improvement in parameter efficiency and generally provides good performance on downstream tasks. Another common approach is to freeze the image encoder and fine-tune the entire mask decoder. This is because the cross-attention layers in the decoder focus on specific patches in the image embeddings corresponding to the prompts and transform them into segmentation predictions [31]. We call this approach DecFT, where  $\theta_{\text{MD}}$  is updated. It is also possible to freeze all the parameters and fine-tune only the output layers, namely, UP and HYP. This approach is analogous to linear probing in classification tasks, which we refer to as partial decoder fine tuning (PDecFT). Since only a small fraction of parameters, namely,  $\theta_{\text{MD-UP}}$ , and  $\theta_{\text{MD-HYP}}$  are updated, PDecFT has high parameter efficiency but usually provides only sub-optimal performance.

**LoRA adapters:** Low-rank adaptation [9] is a promising PEFT technique widely used for adapting foundation models to downstream tasks. Each attention layer within a transformer block has four weight (projection) matrices  $W_q$  (query),  $W_k$  (key),  $W_v$  (value), and  $W_o$  (output), where each  $W \in \mathbb{R}^{d \times d'}$ . The core idea of LoRA is to constrain the modifications to a pre-trained weight matrix  $W$  to a linear update matrix  $\Delta W$ , which can be further constrained using a low-rank decomposition, i.e.,  $\Delta W = BA$ , where  $B \in \mathbb{R}^{d \times r}$ ,  $A \in \mathbb{R}^{r \times d'}$  and the rank  $r \ll \min\{d, d'\}$ . This approach effectively reduces the parameter space while preserving the essential information needed for adaptation.  $W$  is frozen during fine-tuning, and only  $A$  and  $B$  matrices are updated. For input  $x$ , the output  $\tilde{x}$  is computed as follows:

$$\tilde{x} = (W + \alpha\Delta W)x = Wx + \alpha\Delta Wx = Wx + \alpha BAx, \quad (1)$$

where  $\alpha$  is a scale parameter. Following [9], we employ LoRA only to the projection matrices  $W_q$  and  $W_v$  in all the  $\Gamma$  attention layers of IE and MD. Let  $\theta_{\text{LoRA}}$  represent the set of all LoRA parameters, where  $\theta_{\text{LoRA}} = \{A_q^\ell, A_v^\ell, B_q^\ell, B_v^\ell\}_{\ell=1}^\Gamma$ . When only the LoRA parameters are updated during fine-tuning, we refer to this case as LoRAFT. While this approach also has good parameter efficiency, it typically results in sub-optimal performance for segmentation tasks. To improve this, in SAMed[32], both the decoder and LoRA are fine-tuned. Here,  $\theta_{\text{MD}}$  and  $\theta_{\text{LoRA}}$  parameters are updated together, and we represent this approach as LoRADecFT.

**Federated Learning:** In an FL system,  $K$  clients can collaboratively train a global model with parameters  $\Theta$ . The goal is to solve the following optimization problem:

$$\min_{\Theta \in \mathbb{R}^T} \frac{1}{K} \sum_{k=1}^K \mathcal{L}_k^{seg}(\Theta), \quad (2)$$

where  $\mathcal{L}_k^{seg}(\Theta) = E_{x \sim \mathcal{D}_k}[\mathcal{L}_k^{seg}(\Theta; x)]$  is the loss function of the  $k^{th}$  client ( $k \in [1, K]$ ),  $\mathcal{D}_k$  represents the data distribution of the  $k^{th}$  client, and  $T = |\Theta|$  is the number of parameters that need to be learned. Note that if the distributions  $\mathcal{D}_i$  and  $\mathcal{D}_j$  are different for clients  $i$  and  $j$ , the scenario is referred to as non-iid (not independent and identically distributed). A widely used method for solving the optimization problem is FedAvg [21]. At each round, the server broadcasts the global model to each client. Then, all clients conduct local training on their data and send back the updated model to the server. Finally, the server updates the global model as a weighted average of these local model updates. The server update at round  $n$  in FedAvg can be formulated as follows:

$$\Theta^{n+1} = \sum_{k=1}^K \alpha_k \Theta_k^n, \quad (3)$$

where  $\Theta_k^n$  denotes the local model of  $k^{th}$  client in round  $n$  and  $\alpha_k$  is the weight assigned for each client.

### 3 Proposed FLAP-SAM Approach

We aim to efficiently and effectively adapt the SAM for medical image segmentation tasks using limited data distributed across multiple entities. Based on this consideration, we propose to update both  $\theta_{\text{LoRA}}$  as well as the final decoder output layers  $\theta_{\text{MD-UP}}$  and  $\theta_{\text{MD-HYP}}$ . This leads to the proposed fine-tuning for SAM, a hybrid of PDecFT and LoRAFT, as shown in Fig 2. Though there is a marginal increase in the number of parameters compared to LoRAFT, the proposed approach performs well because FLAP-SAM provides enough flexibility to be effectively fine-tuned. Moreover, since almost all the parameters of the original foundation model are retained without modification, its inherent capabilities remain unaffected. Another benefit is its memory efficiency, and the small parameter size of the proposed adapter makes it possible to learn them collaboratively via FL while greatly reducing communication costs.

When aggregating LoRA parameters ( $\theta_{\text{LoRA}}$ ), the  $k^{th}$  client sends  $\{A_{q,k}^\ell, A_{v,k}^\ell, B_{q,k}^\ell, B_{v,k}^\ell\}_{\ell=1}^{\Gamma}$  to the server. The server first needs to reconstruct  $\Delta W_{q,k}^\ell = B_{q,k}^\ell \cdot A_{q,k}^\ell$  and  $\Delta W_{v,k}^\ell = B_{v,k}^\ell \cdot A_{v,k}^\ell$  for each  $\ell$  and  $k$ , then performs FedAvg as shown in Eq. (3) to get the aggregated global weight matrices  $\Delta W_q^\ell$  and  $\Delta W_v^\ell$  of each attention layer  $\ell$ . Finally, the server applies singular value decomposition to decompose the aggregated matrices back to global LoRA parameters  $\{A_q^\ell, B_q^\ell, A_v^\ell, B_v^\ell\}_{\ell=1}^{\Gamma}$ , which are sent back to the clients. We refer to this federated learning of plug-and-play SAM adapter as FLAP-SAM.

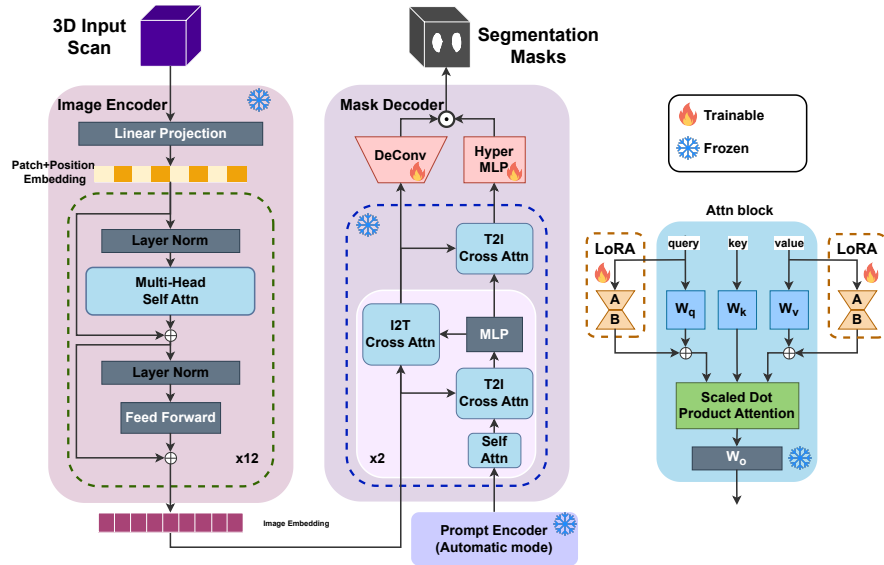


**Fig. 2.** Architecture of the proposed plug-and-play adapter. Only the decoder output layers and LoRAs are fine-tuned, while the remaining parameters in SAM are frozen.

## 4 Experiments

**Datasets:** We utilize *Fed-KITS2019*, a 6-client federated version of the KiTS19 dataset from FLamby [26], which was created from the Kidney Tumor Segmentation Challenge 2019 in CT scans [7,8]. Each client’s train/test split is 9/3, 11/3, 9/3, 9/3, 12/4, and 24/6. The preprocessing pipeline comprises intensity clipping (5<sup>th</sup> and 95<sup>th</sup> percentile of image intensities of each client were calculated) followed by z-scale normalization, where we subtract the mean and divide by the standard deviation of the image intensities. *Fed-IXI*, extracted from the Information eXtraction from Images - IXI database [23,25] of brain T1 MRIs from 3 hospitals (Guys, HH, and IOP) contains 249/62, 145/36 and 59/15 train/test splits respectively. In a preprocessing step, min-max normalization was applied to each scan and padded with zeros in the axial plane (final shape  $83 \times 64 \times 64$ ). *Prostate MRI* is a multi-site segmentation dataset proposed by Liu *et al.* [18], comprises prostate T2-weighted MRI data from six different data sources (*i.e.*, Site A to F) out of the three publicly available datasets: NCI-ISBI13 dataset [1], I2CVB dataset [15] and PROMISE12 dataset [17]. Each site has 30, 30, 19, 13, 12, 12 MRI scans of patients respectively and were randomly divided into train ( $\approx 80\%$ ) and test ( $\approx 20\%$ ) sets. Since they were acquired with varying imaging protocols and contain heterogeneous data distributions, we normalized each site to zero mean and unit variance to reduce the intensity variance among different sites. We resized it to  $224 \times 224$  in the axial plane.

**Table 1.** Comparison on all datasets for different fine-tuning methods. ‡– FL setting of MA-SAM is not feasible since decomposing FacT tensors after aggregation is not possible; a centralized score is provided for performance comparison in 3D segmentation. \*\* – Parameter counts for single class segmentation task (add 0.134M params for each additional class). The baseline (full fine-tuning) is highlighted in Blue and our method in Pink.

Experiments	Setting	Mean Dice score			Trainable/
		Fed-KiTS	Fed-IXI	Prost.MRI	Total params**
<b>FullFT</b> (baseline) $\{\theta_{IE}, \theta_{PE}, \theta_{MD}\}$	Local	0.4493	0.9777	0.8421	
	Federated	0.5444	0.9811	0.9084	90.399M/90.399M
	Centralized	0.5274	0.9834	0.8955	(100%)
<b>AttnFT</b> $\{\theta_{IE-AT}, \theta_{MD}\}$	Local	0.4838	0.8848	0.6315	
	Federated	0.5724	0.9674	0.8797	29.575M/90.399M
	Centralized	0.5486	0.9774	0.8957	(32.7%)
<b>DecFT</b> $\{\theta_{MD}\}$	Local	0.4213	0.9750	0.8200	
	Federated	0.5068	0.9771	0.8101	3.768M/90.399M
	Centralized	0.5179	0.9789	0.8587	(4.2%)
<b>LoRAFT</b> $\{\theta_{LoRA}\}$	Local	0.3717	0.9728	0.8386	
	Federated	0.3687	0.9777	0.8578	1.368M/91.767M
	Centralized	0.5242	0.9798	0.8893	(1.5%)
<b>LoRADecFT</b> (SAMed)[20] $\{\theta_{LoRA}, \theta_{MD}\}$	Local	0.5053	0.9829	0.8929	
	Federated	0.5987	0.9836	0.8949	5.270M/91.767M
	Centralized	0.6100	0.9852	0.9039	(5.8%)
<b>PDecFT</b> $\{\theta_{UP}, \theta_{HYP}\}$	Local	0.3764	0.9678	0.7890	
	Federated	0.4536	0.9693	0.7017	0.344M/90.399M
	Centralized	0.4793	0.9711	0.8008	(0.4%)
<b>FLAP-SAM</b> (ours) $\{\theta_{LoRA}, \theta_{UP}, \theta_{HYP}\}$	Local	0.5069	0.9829	0.8845	
	Federated	0.6046	0.9834	0.8867	1.712M/91.767M
	Centralized	0.5980	0.9851	0.9044	(1.9%)
<b>MA-SAM</b> ‡[2]	Centralized	0.6023	0.9707	0.9125	28.667M/115.298M (25%)

**Implementation details:** We follow the input format and data augmentation as described in [2], conducting all experiments using the “vit\_b” version of SAM on an NVIDIA A100-SXM4-40GB GPU. The input to the model is of size  $(N \times H \times W)$ , which consists of every set of  $N$  consecutive slices ( $N = 5$ ). In LoRA, we initialize matrix  $A$  from a random Gaussian distribution while setting matrix  $B$  to zero and rank to 32. The fine-tuning process employs a hybrid segmentation loss, combining cross-entropy loss and Dice loss as  $\mathcal{L}^{seg} = \alpha \mathcal{L}^{CE} + \beta \mathcal{L}^{Dice}$ , with weighting factors  $\alpha = 0.2$  and  $\beta = 0.8$  following [32]. The training utilizes the Adam optimizer with a batch size of 32. We compare federated learning with localized (using client-owned data alone) and centralized

(all data pooled) settings. We test each site data separately for all fine-tuning strategies, and the results are tabulated in Table 1.

**Table 2.** Average Dice score across local test data in the federated setting on Fed-KiTS19 dataset. (Left) different rank values of LoRA; (Right) different low-rank adapter methods.

LoRA rank	Mean Dice	Trainable / Total params	Adapter	Mean Dice	Trainable / Total params
<b>32</b>	<b>0.605</b>	1.846M/91.901M	<b>LoRA</b>	<b>0.605</b>	1.846M/91.901M
<b>16</b>	0.599	1.162M/91.217M	<b>DoRA</b>	0.592	1.846M/91.901M
<b>4</b>	0.600	0.649M/90.704M	<b>MoLE</b>	0.603	4.583M/94.637M

#### 4.1 Results and Discussion

Our proposed FLAP-SAM method achieves 6% absolute improvement in Dice score compared to the FullFT approach, with a  $\sim 49\times$  reduction in communication overhead on Fed-KiTS. Due to the small size of the dataset, the FullFT approach easily results in overfitting, highlighting the importance of using PEFT methods in limited data settings [3]. The Attention fine-tuning (AttnFT) only achieves half of our improvement (2.8% less than FLAP-SAM) and still incurs  $\sim 17\times$  more communication cost than our method. Both LoRAFT and PDecFT are more efficient but have lower Dice scores than our method. The LoRADecFT achieves an equivalent dice score to our method, but our method is  $\sim 2.8\times$  more efficient regarding parameters and communication. We conduct ablation on the rank parameter of LoRA in FL, and the results are shown in Table 2. We observe that a lower LoRA rank significantly reduces the trainable parameters with a marginal degradation in the Dice score. We also conduct experiments with other low-rank adapters like DoRA[19] and MoLE[30], which only show marginal performance differences among the adapters.

We also benchmark FLAP-SAM against MA-SAM [2], which uses a 3D adapter along with FacT for fine-tuning. We perform this comparison only in the centralized setting because the decomposition of  $\Delta W$  back to FacT-Tensor-Train or FacT-Tucker formats [13] after federated aggregation is not straightforward. Although MA-SAM produces comparable results to our method (see Table 1) in a centralized setting, it uses 28.7M trainable parameters ( $\sim 16\times$  more than our method). This validates our choice of using LoRA, which is both parameter-efficient and FL-friendly.

## 5 Conclusion

In this work, we have tackled adapting a foundational segmentation model (SAM) for 3D medical image segmentation by incorporating an effective PEFT



strategy. We critically analyze the LoRA adapter’s impact and various SAM components to make the fine-tuning for dense 3D segmentation tasks amenable to FL. Our approach simultaneously addresses data scarcity, overfitting, and communication overhead challenges, resulting in a practical and cost-efficient solution. Our current work analyses various fine-tuning methods in the context of FedAVG[21]; an interesting future direction would be studying the effects of various federated optimization strategies on low-rank adapters for datasets with considerable distribution shifts.

**Disclosure of Interests.** The authors have no competing interests to declare that are relevant to the content of this article.

## References

1. Bloch, N., Madabhushi, A., Huisman, H., Freymann, J., Kirby, J., Grauer, M., Enquobahrie, A., Jaffe, C., Clarke, L., Farahani, K.: Nci-isbi 2013 challenge: automated segmentation of prostate structures. *The Cancer Imaging Archive* **370**(6), 5 (2015)
2. Chen, C., Miao, J., Wu, D., Yan, Z., Kim, S., Hu, J., Zhong, A., Liu, Z., Sun, L., Li, X., et al.: Ma-sam: Modality-agnostic sam adaptation for 3d medical image segmentation. *arXiv preprint arXiv:2309.08842* (2023)
3. Chen, G., Liu, F., Meng, Z., Liang, S.: Revisiting parameter-efficient tuning: Are we really there yet? In: *Proceedings of the 2022 Conference on Empirical Methods in Natural Language Processing*. pp. 2612–2626 (2022)
4. Cheng, D., Qin, Z., Jiang, Z., Zhang, S., Lao, Q., Li, K.: Sam on medical images: A comprehensive study on three prompt modes. *arXiv preprint arXiv:2305.00035* (2023)
5. Dosovitskiy, A., Beyer, L., Kolesnikov, A., Weissenborn, D., Zhai, X., Unterthiner, T., Dehghani, M., Minderer, M., Heigold, G., Gelly, S., Uszkoreit, J., Houshy, N.: An image is worth 16x16 words: Transformers for image recognition at scale. In: *ICLR* (2021)
6. He, S., Bao, R., Li, J., Grant, P.E., Ou, Y.: Accuracy of segment-anything model (sam) in medical image segmentation tasks. *arXiv preprint arXiv:2304.09324* (2023)
7. Heller, N., Isensee, F., Maier-Hein, K.H., Hou, X., Xie, C., Li, F., Nan, Y., Mu, G., Lin, Z., Han, M., et al.: The state of the art in kidney and kidney tumor segmentation in contrast-enhanced ct imaging: Results of the kits19 challenge. *Medical Image Analysis* p. 101821 (2020)
8. Heller, N., Sathianathan, N., Kalapara, A., Walczak, E., Moore, K., Kaluzniak, H., Rosenberg, J., Blake, P., Rengel, Z., Oestreich, M., et al.: The kits19 challenge data: 300 kidney tumor cases with clinical context, ct semantic segmentations, and surgical outcomes. *arXiv preprint arXiv:1904.00445* (2019)
9. Hu, E.J., Shen, Y., Wallis, P., Allen-Zhu, Z., Li, Y., Wang, S., Wang, L., Chen, W.: LoRA: Low-rank adaptation of large language models. In: *ICLR* (2022)
10. Huang, Y., Yang, X., Liu, L., Zhou, H., Chang, A., Zhou, X., Chen, R., Yu, J., Chen, J., Chen, C., Liu, S., Chi, H., Hu, X., Yue, K., Li, L., Grau, V., Fan, D.P., Dong, F., Ni, D.: Segment anything model for medical images? *Medical Image Analysis* **92**, 103061 (2024)

11. Huix, J.P., Ganeshan, A.R., Haslum, J.F., Söderberg, M., Matsoukas, C., Smith, K.: Are natural domain foundation models useful for medical image classification? In: Proceedings of the IEEE/CVF Winter Conference on Applications of Computer Vision. pp. 7634–7643 (2024)
12. Jia, M., Tang, L., Chen, B.C., Cardie, C., Belongie, S., Hariharan, B., Lim, S.N.: Visual prompt tuning. In: ECCV. pp. 709–727. Springer (2022)
13. Jie, S., Deng, Z.H.: Fact: Factor-tuning for lightweight adaptation on vision transformer. In: Proceedings of the AAAI Conference on Artificial Intelligence. vol. 37, pp. 1060–1068 (2023)
14. Kirillov, A., Mintun, E., Ravi, N., Mao, H., Rolland, C., Gustafson, L., Xiao, T., Whitehead, S., Berg, A.C., Lo, W.Y., et al.: Segment anything. In: ICCV. pp. 4015–4026 (2023)
15. Lemaître, G., Martí, R., Freixenet, J., Vilanova, J.C., Walker, P.M., Meriaudeau, F.: Computer-aided detection and diagnosis for prostate cancer based on mono and multi-parametric mri: A review. *Computers in Biology and Medicine* **60**, 8–31 (2015)
16. Li, T., Sahu, A.K., Zaheer, M., Sanjabi, M., Talwalkar, A., Smith, V.: Federated optimization in heterogeneous networks. *Proceedings of Machine learning and systems* **2**, 429–450 (2020)
17. Litjens, G., Toth, R., Van De Ven, W., Hoeks, C., Kerkstra, S., Van Ginneken, B., Vincent, G., Guillard, G., Birbeck, N., Zhang, J., et al.: Evaluation of prostate segmentation algorithms for mri: the promise12 challenge. *Medical image analysis* **18**(2), 359–373 (2014)
18. Liu, Q., Dou, Q., Heng, P.A.: Shape-aware meta-learning for generalizing prostate mri segmentation to unseen domains. In: MICCAI (2020)
19. Liu, S.Y., Wang, C.Y., Yin, H., Molchanov, P., Wang, Y.C.F., Cheng, K.T., Chen, M.H.: Dora: Weight-decomposed low-rank adaptation. arXiv preprint arXiv:2402.09353 (2024)
20. Ma, J., He, Y., Li, F., Han, L., You, C., Wang, B.: Segment anything in medical images. *Nature Communications* **15**(1), 654 (2024)
21. McMahan, B., Moore, E., Ramage, D., Hampson, S., y Arcas, B.A.: Communication-efficient learning of deep networks from decentralized data. In: Artificial intelligence and statistics. pp. 1273–1282. PMLR (2017)
22. Paranjape, J.N., Nair, N.G., Sikder, S., Vedula, S.S., Patel, V.M.: Adaptivesam: Towards efficient tuning of sam for surgical scene segmentation. arXiv preprint arXiv:2308.03726 (2023)
23. Pérez-García, F., Sparks, R., Ourselin, S.: Torchio: a python library for efficient loading, preprocessing, augmentation and patch-based sampling of medical images in deep learning. *Computer Methods and Programs in Biomedicine* **208**, 106236 (2021)
24. Ronneberger, O., Fischer, P., Brox, T.: U-net: Convolutional networks for biomedical image segmentation. In: MICCAI 2015: 18th International Conference, Munich, Germany, October 5–9, 2015, Proceedings, Part III 18. pp. 234–241. Springer (2015)
25. Team, B.D.: Ixi-dataset, <https://brain-development.org/ixi-dataset/>
26. Ogier du Terrail, J., Ayed, S.S., Cyffers, E., Grimberg, F., He, C., Loeb, R., Mangold, P., Marchand, T., Marfoq, O., Mushtaq, E., et al.: Flamby: Datasets and benchmarks for cross-silo federated learning in realistic healthcare settings. *Advances in Neural Information Processing Systems* **35**, 5315–5334 (2022)
27. Touvron, H., Cord, M., El-Nouby, A., Verbeek, J., Jégou, H.: Three things everyone should know about vision transformers. In: European Conference on Computer Vision. pp. 497–515. Springer (2022)

28. Wang, A., Islam, M., Xu, M., Zhang, Y., Ren, H.: Sam meets robotic surgery: An empirical study in robustness perspective. arXiv preprint arXiv:2304.14674 (2023)
29. Wu, J., Fu, R., Fang, H., Liu, Y., Wang, Z., Xu, Y., Jin, Y., Arbel, T.: Medical sam adapter: Adapting segment anything model for medical image segmentation. arXiv preprint arXiv:2304.12620 (2023)
30. Wu, X., Huang, S., Wei, F.: Mole: Mixture of lora experts. In: The Twelfth International Conference on Learning Representations (2023)
31. Xie, W., Willems, N., Patil, S., Li, Y., Kumar, M.: Sam fewshot finetuning for anatomical segmentation in medical images. In: Proceedings of the IEEE/CVF Winter Conference on Applications of Computer Vision. pp. 3253–3261 (2024)
32. Zhang, K., Liu, D.: Customized segment anything model for medical image segmentation. arXiv preprint arXiv:2304.13785 (2023)
33. Zhang, S., Metaxas, D.: On the challenges and perspectives of foundation models for medical image analysis. *Medical Image Analysis* **91**, 102996 (2024)





**Table C.** Results on Fed-IXI dataset for different fine-tuning methods. ‡– FL setting of MA-SAM is not shown due to challenges in decomposing FacT tensors after federated aggregation. The baseline (full fine-tuning) is highlighted in **Blue** and our method in **Pink**. The best and second best methods for FL are highlighted in **bold** and underline, respectively.

Experiments (Trainable/Total params)	Setting	Dice score			
		SiteA	SiteB	SiteC	Average
<b>FullFT (Baseline)</b> $\{\theta_{IE}, \theta_{PE}, \theta_{MD}\}$ (90.399M/90.399M) 100%	Local	0.9808	0.9797	0.9728	0.9777
	Federated	0.9837	0.9835	0.9761	0.9811
	Centralized	0.9838	0.9846	0.9818	0.9834
<b>AttnFT</b> $\{\theta_{IE-AT}, \theta_{MD}\}$ (29.575M/90.399M) 32.7%	Local	0.9592	0.9708	0.7244	0.8848
	Federated	0.9713	0.9701	0.9608	0.9674
	Centralized	0.9781	0.9791	0.9749	0.9774
<b>DecFT</b> $\{\theta_{MD}\}$ (3.768M/90.399M) 4.2%	Local	0.9783	0.9787	0.9680	0.9750
	Federated	0.9780	0.9787	0.9746	0.9771
	Centralized	0.9791	0.9806	0.9770	0.9789
<b>LoRAFT</b> $\{\theta_{LoRA}\}$ (1.368M/91.767M) 1.5%	Local	0.9788	0.9776	0.9620	0.9728
	Federated	0.9790	0.9791	0.9749	0.9777
	Centralized	0.9803	0.9808	0.9785	0.9798
<b>LoRADecFT</b> $\{\theta_{MD}, \theta_{LoRA}\}$ (5.136M/91.767M) 5.7%	Local	0.9850	0.9853	0.9784	0.9829
	Federated	<b>0.9850</b>	<b>0.9853</b>	<b>0.9806</b>	<b>0.9836</b>
	Centralized	0.9855	0.9864	0.9837	0.9852
<b>PDecFT</b> $\{\theta_{UP}, \theta_{HYP}\}$ (0.344M/90.399M) 0.4%	Local	0.9713	0.9722	0.9600	0.9678
	Federated	0.9697	0.9725	0.9658	0.9693
	Centralized	0.9718	0.9729	0.9685	0.9711
<b>FLAP-SAM (Ours)</b> $\{\theta_{LoRA}, \theta_{UP}, \theta_{HYP}\}$ (1.712M/91.767M) 1.9%	Local	0.9850	0.9849	0.9788	0.9829
	Federated	<u>0.9847</u>	<u>0.9852</u>	<u>0.9803</u>	<u>0.9834</u>
	Centralized	0.9854	0.9864	0.9835	0.9851
<b>MA-SAM<sup>‡</sup></b> (28.667M/115.297M) 25%	Centralized	0.972	0.972	0.968	0.971

**Table D.** Results across local site test data for different rank values of LoRA in the federated setting on Fed-KiTS19 dataset.

LoRA rank	Dice score							Trainable / Total params
	SiteA	SiteB	SiteC	SiteD	SiteE	SiteF	Average	
<b>32</b>	0.723	0.577	0.617	0.555	0.576	0.579	0.605	1.846M / 91.901M
<b>16</b>	0.720	0.572	0.616	0.518	0.561	0.604	0.599	1.162M / 91.217M
<b>4</b>	0.703	0.590	0.609	0.538	0.588	0.572	0.600	0.649M / 90.704M

**Table E.** Results across local test data site for different PEFT methods in the federated setting on Fed-KiTS19 dataset.

Methods	Dice score							Trainable / Total params
	SiteA	SiteB	SiteC	SiteD	SiteE	SiteF	Average	
<b>LoRA</b>	0.723	<b>0.577</b>	<b>0.617</b>	<b>0.555</b>	0.576	0.578	<b>0.605</b>	1.846M / 91.901M
<b>DoRA</b>	<b>0.725</b>	0.470	0.615	0.537	0.609	0.594	0.592	1.846M / 91.901M
<b>MoLE</b>	0.712	0.517	0.613	0.552	<b>0.615</b>	<b>0.611</b>	0.603	4.583M / 94.637M